Antiviral Research 87 (2010) 213–222

Contents lists available at ScienceDirect

Antiviral Research

journal homepage: www.elsevier.com/locate/antiviral

Biochemical characterization of the inhibition of the dengue virus RNA polymerase by beta-D-2′-ethynyl-7-deaza-adenosine triphosphate

Derek R. Latour, Andreas Jekle, Hassan Javanbakht, Robert Henningsen, Peter Gee, Ina Lee, Patricia Tran, Suping Ren, Alan K. Kutach, Seth F. Harris, Sandra M. Wang, Stephen J. Lok, David Shaw, Jim Li, Gabrielle Heilek, Klaus Klumpp, David C. Swinney*, Jerome Deval**

Roche Palo Alto LLC, 3431 Hillview Avenue, Palo Alto, CA, United States

ARTICLE INFO

Article history:
Received 4 January 2010
Received in revised form 30 April 2010
Accepted 5 May 2010

Keywords:
Dengue virus
NS5 polymerase
Nucleotide
Chain terminator
Single-nucleotide incorporation
Steady-state kinetics

ABSTRACT

Dengue virus (DENV), an emerging pathogen from the *Flaviviridae* family with neither vaccine nor antiviral treatment available, causes a serious worldwide public health threat. In theory, there are several ways by which small molecules could inhibit the replication cycle of DENV. Here, we show that the nucleoside analogue beta-D-2′-ethynyl-7-deaza-adenosine inhibits representative strains of all four serotypes of DENV with an EC_{50} around or below 1 μM. Using membrane-associated native replicase complex as well as recombinant RNA polymerase from each DENV serotype in enzymatic assays, we provide evidence that beta-D-2′-ethynyl-7-deaza-adenosine triphosphate (2′E-7D-ATP) targets viral replication at the polymerase active site by competing with the natural nucleotide substrate with an apparent K_i of 0.060 ± 0.016 μM. In single-nucleotide incorporation experiments, the catalytic efficiency of 2′E-7D-ATP is 10-fold lower than for natural ATP, and the incorporated nucleotide analogue causes immediate chain termination. A combination of bioinformatics and site-directed mutagenesis demonstrates that 2′E-7D-ATP is equipotent across all serotypes because the nucleotide binding site residues are conserved in dengue virus. Overall, beta-D-2′-ethynyl-7-deaza-adenosine provides a promising scaffold for the development of inhibitors of dengue virus polymerase.

1. Introduction

The *Flaviviridae* virus family includes important human pathogens such as hepatitis C virus (HCV), dengue virus (DENV), West Nile virus (WNV), and yellow fever virus (YFV). Dengue virus is spread by the mosquito *Aedes aegypti* and causes an acute fever sometimes followed by hemorrhage (or plasma leakage) and shock syndrome in secondary infections. Dengue virus infects 50–100 million individuals per year through explosive waves of epidemics in the tropical and sub-tropical regions of the world (Halstead, 2007). The genome of DENV contains roughly 11,000 nucleotides of a positive single-stranded RNA that encodes a single polyprotein. The proteolytic cleavage of this precursor results in the releases of 10 structural and non-structural proteins necessary for assembly and release of infectious virus progeny.

The idea of targeting the non-structural proteins of dengue virus with antivirals has recently emerged (Bollati et al., 2009; Ray and Shi, 2006; Sampath and Padmanabhan, 2009). A potentially attractive target for the development of such inhibitors is the non-structural protein 5 (NS5), the largest of the DENV proteins. NS5 is essential for replication of the dengue viral genome. The 900 amino acid protein contains a (guaninine-N7) and (nucleoside-2′-O-) methyltransferase (MTase) domain at its N-terminus and a RNA-dependent-RNA polymerase (RdRp) domain at the C-terminus (Bollati et al., 2009; Brooks et al., 2002; Pryor et al., 2007; Yap et al., 2007). The RdRp domain duplicates the viral genome in a linear and continuous manner, starting from the 3′-end of the single-stranded RNA (ssRNA) template. Initiation of RNA synthesis by polymerases from the *Flaviviridae* family is primer-independent, meaning that the viral enzymes have to generate their own primer prior to reaching the processive elongation mode (Ackermann and Padmanabhan, 2001; van Dijk et al., 2004). As seen in HCV, bovine viral diarrhea virus (BVDV), and WNV, the DENV polymerase adopts a typical right-hand structure featuring three subdomains: fingers, palm, and thumb. (Bressanelli et al., 1999; Choi et al., 2004; Malet

Abbreviations: AMP, adenosine monophosphate; ATP, adenosine triphosphate; BVDV, Bovine viral diarrhea virus; CPE, cytopathic effect; DENV, dengue virus; HCV, hepatitis C virus; IU, international unit; MTase, methyltransferase; NS5, non-structural protein 5; NS5pol, polymerase domain of NS5; FL, full length; NGC, new Guinea C; ssRNA, single-stranded RNA; YFV, yellow fever virus; WNV, West Nile virus; 2′E-7D-ATP, beta-D-2′-ethynyl-7-deaza-adenosine triphosphate.

* Corresponding author. Tel.: +1 650 855 5349; fax: +1 650 852 1700.
** Corresponding author. Tel.: +1 650 855 6958; fax: +1 650 852 1700.
E-mail addresses: david.swinney@roche.com (D.C. Swinney), jeromedeval@hotmail.com (J. Deval).

0166-3542/$ – see front matter © 2010 Elsevier B.V. All rights reserved.
doi:10.1016/j.antiviral.2010.05.003

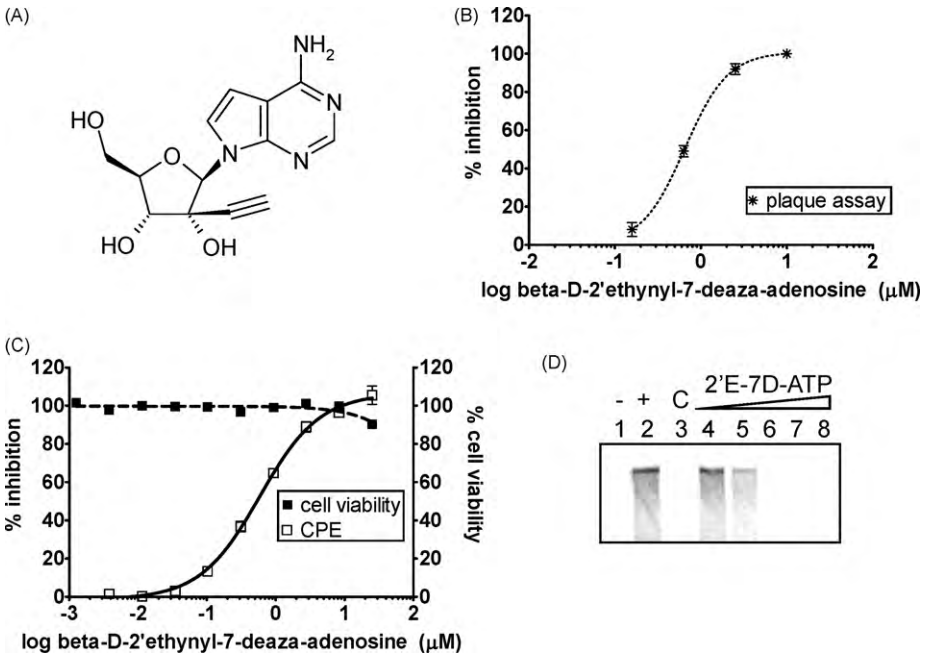

Fig. 1. Antiviral activity of beta-D-2′-ethynyl-7-deaza-adenosine against dengue virus. (A) Chemical structure of beta-D-2′-ethynyl-7-deaza-adenosine. (B) Inhibition of DENV-3 replication by beta-D-2′-ethynyl-7-deaza-adenosine is followed indirectly in a standard plaque assay. Protection of BHK-21 cells from virus-induced cytopathic effect is monitored in the presence of four serial dilutions of beta-D-2′-ethynyl-7-deaza-adenosine (10, 2.5, 0.6, and 0.2 μM). (C) Inhibition of virus-induced cytopathic effect (CPE) in Huh-7 cells, by increasing concentrations of beta-D-2′-ethynyl-7-deaza-adenosine up to 25 μM. Cell viability was monitored with the same compound concentration range in uninfected cells. (D) Inhibition of the polymerase activity of membrane-associated native replicase of DENV by 2′E-7D-ATP. The membrane fraction from Vero cells containing a stable DENV-2 replicon was incubated for 2 h in the presence of all four NTPs including 1 μM ATP and radiolabeled ^{33}P-CTP as tracer (lane 2), and 50 μM of the chain terminator 3'dATP was chosen as inhibitor control of the polymerase activity (lane 3). Lanes 4–8: increasing concentrations of 2′E-7D-ATP were added to the polymerase reaction, lane 4: 0.08 μM, lane 5: 0.4 μM, lane 6: 2 μM, lane 7: 10 μM, and lane 8: 50 μM.

et al., 2007; Yap et al., 2007). In the absence of an elongated primer, the polymerase domain adopts a close conformation where fingers and thumb are connected. Therefore, significant conformational changes are likely to take place within these subdomains in order for the enzyme to transition from the initiation to the elongation step, offering multiple opportunities by which a small molecule can have a pharmacological effect.

Nucleoside analogues are widely validated for antiviral therapies. These molecules have been clinically tested or approved against herpesvirus and cytomegalovirus, hepatitis B and C viruses, HIV, and influenza (De Clercq and Neyts, 2009). Most nucleosides inhibit viral polymerases in the cytoplasm by the process of chain termination, in which the incorporation of the nucleotide analogue stops nucleic acid synthesis. These analogues must be transported into the infected cell and converted to the active triphosphate by cellular kinases in order to inhibit viral polymerases by chain termination.

In this study, we provide a detailed biochemical characterization of the inhibition of dengue virus polymerase by the nucleotide analogue beta-D-2′-ethynyl-7-deaza-adenosine triphosphate (2′E-7D-ATP). First, we investigated at the cell-based level the antiviral potency of beta-D-2′-ethynyl-7-deaza-adenosine (Fig. 1A), a novel 2′-modified nucleoside with anti-dengue virus properties (Yin et al., 2009, 2008). We showed that 2′E-7D-ATP inhibits the polymerase activity of membrane-associated DENV replicase complex, which explains the antiviral potency of the parent nucleoside against representative strains of the four serotypes. In order to further characterize the mode of inhibition of 2′E-7D-ATP, we produced the corresponding recombinant NS5 for each DENV serotype and measured their intrinsic polymerase activity by steady-state kinetics. We observed significant heterogeneity in catalytic efficiency (1) between the polymerase domain and the full-length NS5, and (2) across serotypes. Most importantly, we found that 2′E-7D-ATP targets dengue virus replication at the polymerase level by first competing with the natural substrate for nucleotide incorporation, followed by immediate chain termination. Overall, this makes beta-D-2′-ethynyl-7-deaza-adenosine the most potent chain terminator of dengue virus polymerase reported to date.

2. Materials and methods

2.1. Chemicals and nucleic acid

The RNA template sequence used in single-nucleotide experiments was chemically synthesized by Integrated DNA Technologies: 5′-UCGUGGCCCAAAAGGGCC-3′ (HP5-A18). The underlined base shows the unique site for incorporation of A-analogues. 5′-end labeling was conducted with [γ^{33}P] ATP and T4 polynucleotide kinase according to manufacturer's recommendation (Invitrogen). After inactivation of the kinase by heat, the radiolabeled RNA was purified with G25 spin columns (GE healthcare). The minus strand 3′UTR RNA was synthesized with the T7 Megascript kit (Ambion), using the last 380 bases from the negative strand of the DENV serotype 2 New Guinea C (NGC strain) genome as template. 3′-dATP was purchased from TriLink Biotechnologies. Beta-D-2′-ethynyl-7-deaza-adenosine adenosine was synthesized in-house (94.6% purity) while the corresponding triphosphate was synthesized by TriLink Biotechnologies (95% purity).

2.2. Antiviral assay

Dengue virus representative strains of the four serotypes DENV-1 (Th-Sman), DENV-2 (Th-36), DENV-3 (H-87) and DENV-4 (H-241) were all obtained from the ATCC (Manassas, VA). Virus titers were measured on BHK-21 cells, using a standard plaque assay procedure. For the determination of EC_{50} of nucleoside in the antiviral assay, Huh-7 cells were plated in white 96-well plates in MEM media supplemented with 10% FBS and 1% penicillin/streptomycin.

After incubation for 24 h, cells were infected at a multiplicity of infection (MOI) of 0.5 for 2 h at 37 °C. Ten three-fold dilutions of compounds were prepared in the same media supplemented with 1% DMSO. After the 2 h adsorption phase, virus was aspirated off and diluted compound was added to four wells each. Potential cytotoxicity of compounds on Huh-7 cells was assessed in parallel to the antiviral activity. Huh-7 cells were plated as described above and exposed to the same concentration range of compounds. Untreated cells were carried along as a control. After a 3-day incubation at 37 °C, the cell viability was determined using Cell-titer Glo™ reagent (Promega, Madison, WI) that was added to each well and incubated for 5 min. Plates were analyzed using a Thermo Luminoskan plate reader (Waltham, MA).

2.3. Polymerase activity of membrane-associated replicase complex

Cultured Vero cells containing a stable DENV-2 replicon were ruptured, and cytoplasmic fraction isolation was performed as previously described (Takeda et al., 1986). Briefly, cells were swollen by hypotonic solution at 4 °C before being ruptured by douncing. Nuclei were removed by centrifugation at 1000 × *g*. After another centrifugation step at 30,000 × *g*, cytoplasmic membrane fractions containing the replicase complex were resuspended in 10 mM HEPES pH7.5, 10 mM NaCl, 1 mM DTT, and 15% glycerol. Standard DENV replicase polymerase assay was performed essentially as described for HCV replicase (Ma et al., 2005). The assay contained 6 μL of DENV-2 cytoplasmic membrane fraction, 50 mM HEPES pH. 7.5, 10 mM KCl, 10 mM DTT, 5 mM $MgCl_2$, 200 μM UTP and GTP, 1 μM ATP, 24 μCi [α-^{33}P]–CTP (3000 Ci/mmol, 10 mCi/ml), 20 μg/mL actinomycin D, 1 U/μL SuperaseIn (Ambion), 10 mM creatine phosphate, 200 μg/mL creatine phosphokinase in a final volume of 20 μL. Reactions took place at 30 °C for 2 h and stopped with 50 mM EDTA and 0.5% SDS before the addition of proteinase K for 30 min. Free nucleotides were removed with G-50 columns followed by phenol chloroform extractions and ethanol precipitation of the RNA products. Samples were denatured in glyoxal loading buffer and resolved in a 0.8% agarose – NorthernMax-Gly gel. Gels were dried, scanned on a phosphorimager, and products quantitated using the ImageQuant software (GE Healthcare).

2.4. Expression and purification of recombinant NS5 from four different serotypes of dengue virus

The gene which encodes for the NS5 protein from DENV-2 (NGC strain) was synthesized and sub-cloned into a custom *E. coli* expression vector which was derived from pET11a (Novagen). A sequence of six histidines followed by a thrombin protease cleavage site at the N-terminus of the DENV-2 (NGC) protein was inserted to allow for affinity purification. The NS5 genes derived from DENV-1 (Th-Sman), DENV-3 (H-87) and DENV-4 (H-241), numerically corresponding to the serotype, were sub-cloned from cDNA generated from viral RNA and inserted into a custom Gateway *E. coli* expression vector derived from pDEST17 (Invitrogen). The N-terminus of DENV-1 (Th-Sman), DENV-3 (H-87) and DENV-4 (H-241) proteins contain a 6× His-tag followed by the amino acids translated from the attB1 recombination site and a TEV protease cleavage site. Dengue NS5 proteins were expressed in *E. coli* BL21(DE3) cells by induction with 0.25 mM IPTG for 6 h at 20 °C. Frozen harvested cells were thawed in 4 mL/g of extraction buffer: 25 mM Hepes, pH 7.5, 500 mM NaCl, 10 mM imidazole, 5 mM β-mercaptoethanol, 1 mM TCEP, 10% glycerol, 0.1% Igepal-CA630, 10 U/mL Benzonase (Sigma), and 1× complete EDTA-free protease inhibitors cocktail (Roche). Chromatographic purification of NS5 proteins was performed at 4 °C using ATKAxpress system (GE) using a three step automated purification procedure: NiNTA (Novagen), HiTrap Heparin-Sepharose (GE), and HiLoad Superdex200 (GE). The final buffer was 25 mM Hepes, pH 6.8, 250 mM NaCl, 1 mM TCEP, and 10% glycerol. The protein concentrations were determined by UV280 absorbance, and the identities confirmed by mass spectrometric analysis of tryptic digestion products and intact mass.

2.5. Steady-state kinetics of multiple nucleotide incorporation

Unless otherwise specified, reaction samples consisted of 10 nM (−) 3′UTR RNA and 10 nM NS5, mixed together in a buffer (W7.5) containing 40 mM Tris pH 7.5, 10 mM NaCl, 3 mM DTT, and 2 mM $MgCl_2$ (optimal concentration for enzyme activity). Reactions were started at 30 °C by adding 200 μM ATP, GTP, UTP, and 0.9 μM ^{3}H-CTP (0.5 μCi) in a final volume of 20 μL. The reactions were stopped and RNA was precipitated with 10% trichloroacetic acid for 40 min at 4 °C, prior to filtration on a multiscreen BV 1.2 μm plate (Millipore). Counts were revealed with 30 μL Microscint-20 (PerkinElmer), using a Topcount microplate scintillation reader (PerkinElmer).

2.6. Single-nucleotide incorporation and chain termination reaction

Unless otherwise specified, standard reaction mixtures consisted of 0.2 μM synthetic oligonucleotide RNA (HP5-A18) and 0.2 μM NS5 in the W7.5 buffer. Time course reactions were started at 30 °C by adding ATP, 7-deaza-adenosine triphosphate (7D-ATP), or 2′E-7D-ATP at multiple concentrations, ranging from 3 to 1000 μM. For chain termination experiments, reactions were started by the addition of ATP analogue alone, or in combination with CTP. In all cases, reactions were stopped with formamide (Sigma), followed by heat-denaturation for 5 min at 95 °C, and resolved on 16% polyacrylamide-7 M urea gel, for 2 h at 80 W. Gels were scanned on a phosphorimager, and products quantitated using the ImageQuant software (GE Healthcare).

2.7. Kinetic analysis

All data were analyzed with GraphPad Prism. The apparent Michaelis constant (K_m) of each NTP for NS5 was calculated by nonlinear fitting using the equation $Y = (V_{max} \times X)/(K_m + X)$, where Y corresponds to the rate of RNA synthesis by NS5 (in pmol/min), V_{max} is the maximum rate at saturating substrate concentration, and X corresponds to NTP concentration. The compound concentration at which the enzyme-catalyzed rate was reduced by 50% (IC_{50}) was calculated by fitting the data to the equation $Y = \%Min + (\%Max - \%Min)/(1 + X/IC_{50})$, where Y corresponds to the percent relative enzyme activity, %Min is the residual relative activity at saturating compound concentration, %Max is the relative maximum enzyme activity, and X corresponds to the compound concentration. The IC_{50} value was derived from the mean of a minimum of two independent experiments. The K_i for 3'dATP and for 2′E-7D-ATP was derived by fitting the data to the Cheng–Prusoff equation assuming competitive inhibition relative to AMP incorporation: $K_i = IC_{50}/(1 + [ATP]/K_m)$, where [ATP] is the initial concentration of ATP and K_m is the apparent K_m for ATP.

3. Results

3.1. Antiviral activity of beta-D-2′-ethynyl-7-deaza-adenosine against dengue virus and inhibition of the native replicase complex by the nucleoside triphosphate

We initially used a standard plaque assay to determine the antiviral potency of beta-D-2′-ethynyl-7-deaza-adenosine. We

Table 1
Antiviral activity against four serotypes of dengue virus ($n = 4$).

	EC_{50}				Cell viability
	DENV-1	DENV-2	DENV-3	DENV-4	
Interferon α 2a (IU/mL)	3.27 ± 0.55	1.73 ± 0.15	7.88 ± 3.91	15.41 ± 2.38	92 ± 4% at 100 IU/mL
Beta-D-2′-ethynyl-7-deaza-adenosine (μM)	0.31 ± 0.09	0.69 ± 0.11	1.06 ± 0.37	0.71 ± 0.40	79 ± 5% at 50 μM

measured the protection of BHK-21 cells from the cytopathic effect induced by dengue virus. We observed a dose–response inhibition of plaque formation in the presence of four serial dilutions of beta-D-2′-ethynyl-7-deaza-adenosine, corresponding to the inhibition of cell infection and dengue virus replication (Fig. 1B). Results were confirmed using a higher throughput luciferase assay that monitors cytopathic effect (CPE) by measuring cellular ATP levels in human infected cells (Huh-7). We used interferon α 2a as a positive control of virus inhibition (Table 1). In this assay format, the replication of DENV-2 was inhibited by beta-D-2′-ethynyl-7-deaza-adenosine, with an average EC_{50} of 0.69 ± 0.11 μM (Fig. 1C). We conducted the same experiment with representative strains of the three other dengue virus serotypes, and observed that beta-D-2′-ethynyl-7-deaza-adenosine had an antiviral potency ranging between 0.31 and 1.06 μM (Table 1). Beta-D-2′-ethynyl-7-deaza-adenosine had only a weak effect on cell viability (21% reduction) at concentrations up to 50 μM, the highest tested concentration (Fig. 1C and Table 1).

Since beta-D-2′-ethynyl-7-deaza-adenosine is a ribonucleoside, we suspected that, once converted to the triphosphate form, the nucleotide would directly target the viral replication step at the polymerase level. We therefore purified membrane-associated DENV-2 replicase containing native NS5 in complex with viral genomic RNA. We monitored in a gel-based assay the polymerase activity of the replicase complex by incorporation of a radiolabled nucleotide into nascent RNA (Fig. 1D), following established procedures (Ma et al., 2005; Takeda et al., 1986). Polymerase activity was inhibited by increasing concentration of 2′E-7D-ATP, the triphosphate form of beta-D-2′-ethynyl-7-deaza-adenosine (Fig. 1D, lanes 4–8).

3.2. Purification and kinetic characterization of the recombinant NS5 polymerase of dengue virus

The NS5 protein of dengue virus contains the methyltransferase domain in its N-terminus, followed by the polymerase domain (Fig. 2A). Truncated polymerase domain (NS5pol) and full-length recombinant NS5 from each of the four serotypes of dengue virus were produced in *E. coli*, and purified to at least 95% homogeneity (Fig. 2B). For each enzyme, RNA synthesis under steady-state conditions was measured by following the incorporation of a radiolabeled nucleotide into the growing strand, the resulting product being separated from the free substrate by acidic precipitation and filtration. Time course reactions were started by mixing together 10 nM enzyme with 10 nM RNA in a buffer containing 1 mM $MnCl_2$, the optimal metal ion concentration for enzyme activity (data not shown). Under these conditions, full-length NS5 and NS5pol domain from DENV-2 displayed similar activities (Fig. 2C). However, NS5pol domain showed a significant drop in activity when $MnCl_2$ was replaced by $MgCl_2$. In order to minimize the risk of nucleotide misincorporation and to mimic physiological conditions of RNA polymerization, we decided to use magnesium as the cofactor through the rest of the study in combination with full-length proteins. We next compared the rate of nucleotide polymerization across all four serotypes. Initial velocity was calculated from the amount of product formed during the linear phase, after an

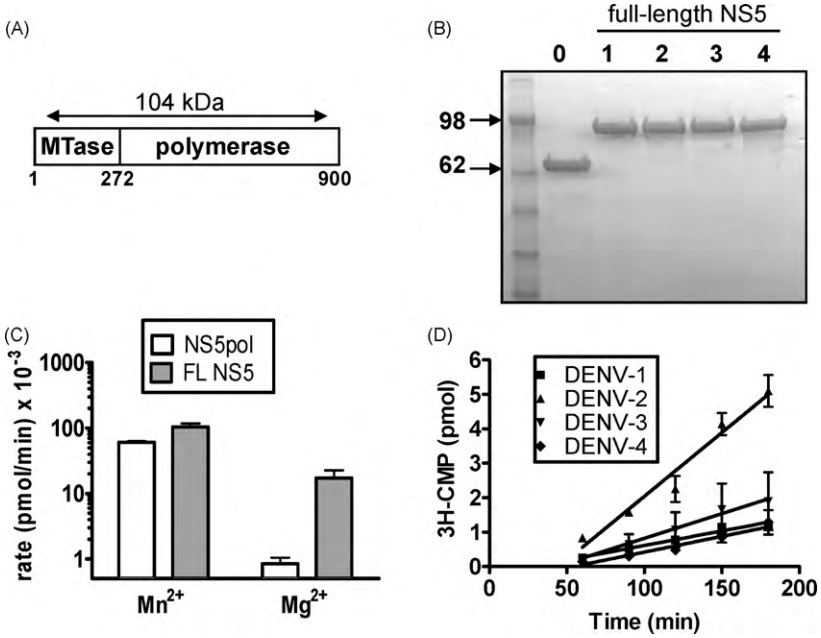

Fig. 2. Purification and initial characterization of the NS5 polymerase of dengue virus. (A) Domain organization of NS5. The methyltransferase (MTase) domain is at the N-terminal a.a. 1–272 followed by the RNA polymerase domain a.a. 273–900. (B) SDS PAGE analysis of purified DENV-2 NS5pol (lane 0), and FL NS5 from four different serotypes (lanes 1–4): type 1: Th-Sman, type 2: NGC, type 3: H-87, type 4: H-241. (C) Comparison of initial velocity of RNA synthesis between full-length NS5 and NS5pol domain of serotype 2, in the presence of either 1 mM $MnCl_2$ or 2 mM $MgCl_2$. Reaction was started by mixing together 10 nM enzyme with 10 nM template and following RNA synthesis over a period of 3 h, using ^{3}H-CTP as a tracer in a radiometric filter-based assay. (D) Progress curve of steady-state polymerase activity of full-length NS5 for all serotypes.

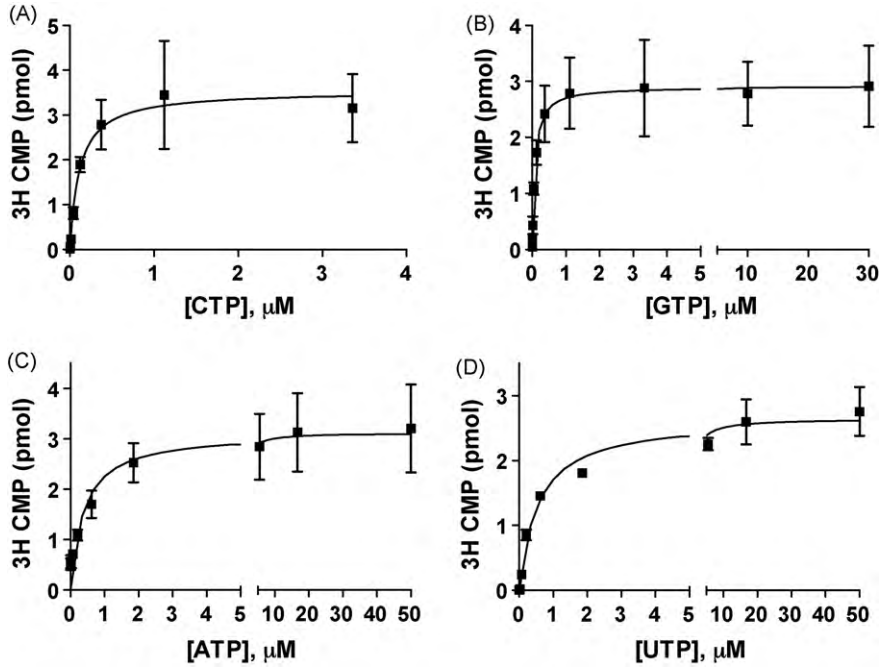

Fig. 3. Steady-state parameters of multiple nucleotide incorporations by DENV-2 NS5. (A) Product versus concentration plot analysis for CTP. The steady-state kinetic constants were derived using the Michaelis–Menten equation, which resulted in K_m(CTP) = 0.12 ± 0.04 μM. (B–D) Same as (A) varying instead the concentration GTP, ATP, or UTP, respectively. The Michaelis–Menten constants for all three nucleotides were: K_m(GTP) = 0.075 ± 0.027 μM, K_m(ATP) = 0.38 ± 0.18 μM, and K_m(UTP) = 0.55 ± 0.01 μM.

initial 30–60-min lag phase (Fig. 2D). High concentrations of CTP did not eliminate the lag (Supplementary information Fig. 1A). We also observed that NS5 from DENV-2 is the most active of the four proteins, with apparent V_{max} in the following ranking order: DENV-2 > DENV-3 > DENV-4 > DENV-1 (Fig. 2D). The same trend in polymerase activity between serotypes was observed using the homopolymeric poly(rA):oligo(rU) RNA substrate (Supplementary information Fig. 1B). Representative Michaelis–Menten plots are shown for the most active DENV-2 NS5 (NGC strain) (Fig. 3A–D), with K_m values for all nucleotides ranging from 0.075 (GTP) to 0.55 μM (UTP). K_m (ATP) values were also measured for the polymerase of each serotype, and the ranking order of specific activity (k_{cat}/K_m) confirmed the initial trend obtained from time course analysis (Table 2).

3.3. 2′E-7D-ATP is a competitive inhibitor of dengue virus polymerase NS5

We next measured the inhibition of the RNA polymerase activity of recombinant NS5 by the triphosphate form of beta-D-2′-ethynyl-7-deaza-adenosine (2′E-7D-ATP). The concentration of natural ATP was reduced to 1 μM (about 2–3 times over K_m), and increasing concentration of nucleotide analogue was added to the polymerase reaction. We used the canonical 3′-dATP as positive control of inhibition as it is an obligate chain terminator with reported inhibitory activity against the closely related HCV polymerase (Olsen et al., 2004). When tested against all four serotypes of dengue virus NS5, the IC_{50} of 3'dATP ranged between 3.1 and 5.8 μM (Table 3). In comparison, 2′E-7D-ATP was 10–15-times more potent across all four serotypes. The methyltransferase domain did not contribute to the observed inhibition, as judged by the IC_{50} of 0.25 ± 0.02 μM against NS5pol domain (Fig. 4A, dotted line). To investigate the mode of inhibition of 2′E-7D-ATP, we also varied the concentration of the natural substrate ATP. The potency of both nucleotide analogues decreased with increasing substrate concentration, which indicates a competitive behavior (Fig. 4B and C). We calculated an average apparent K_i = 0.74 ± 0.072 μM (3′-dATP) and 0.060 ± 0.016 μM (2′E-7D-ATP) using the Cheng–Prusoff equation for each ATP concentration.

3.4. 2′E-7D-ATP is an immediate chain terminator

In order to dissect the mechanism of action of 2′E-7D-ATP, we developed a gel-based assay that measures single-nucleotide incorporation from a preformed enzyme/primer-template complex. In this case, we used a surrogate self-annealing oligonucleotide that can adopt a hairpin structure which allows a single A base incorporation opposite templated U base (Fig. 5A). AMP incorporation was monitored over time by the conversion of the 18-mer substrate to a 19-mer product (Fig. 5B). The reaction was linear for about 20 min, and over 80% complete after 60 min (Fig. 5C). In contrast, the incorporation of 7D-2′E AMP was less than 50%

Table 2
Steady-state kinetic parameters for all four serotypes of dengue polymerase NS5 (n = 2).

	ATP			
	DENV-1	DENV-2	DENV-3	DENV-4
K_m (μM)	0.57 ± 0.13	0.38 ± 0.19	0.51 ± 0.17	0.64 ± 0.14
k_{cat} (min^{-1})	0.0021 ± 0.0002	0.10 ± 0.03	0.029 ± 0.010	0.018 ± 0.003
k_{cat}/K_m (min^{-1} μM^{-1})	0.0040 ± 0.0005	0.28 ± 0.04	0.057 ± 0.001	0.029 ± 0.001
Relative efficiency (%)[a]	1.4	100.0	20.1	10.2

[a] Calculated as $(k_{cat}/K_m)\text{DENV} - n/(k_{cat}/K_m)\text{DENV-2} \times 100$.

Table 3
Inhibitory potency against the four serotypes of dengue polymerase NS5 ($n = 2$).

	IC_{50} (μM)			
	DENV-1	DENV-2	DENV-3	DENV-4
3′-dATP	3.1 ± 0.3	3.4 ± 0.1	4.2 ± 1.4	5.8 ± 1.3
2′E-7D-ATP	0.21 ± 0.08	0.39 ± 0.01	0.36 ± 0.06	0.59 ± 0.13

complete after 60 min. Kinetic constants of single-nucleotide incorporation were calculated for each substrate, which yielded a catalytic efficiency (k_{cat}/K_m) varying from 0.98 ± 0.28 for ATP to 0.096 ± 0.024 min^{-1} mM^{-1} for 2′E-7D-ATP (Fig. 5D). The data suggests that 7D-2′E AMP is incorporated into the viral RNA with approximately 10% of the efficiency of the natural AMP.

We also measured the effect of 7D-2′E AMP at the 3′-end of the primer on the incorporation efficiency of the next correct nucleotide (CTP) at position +2. The addition of CTP alone did not support formation of either 18- or 19-mer (data not shown). When natural AMP was incorporated at position +1, incorporation of the next CMP was fast, as judged by the absence of a visible 19-mer intermediate at any time point (Fig. 5E). 7D-2′E AMP was also efficiently incorporated at the 3′-end of the primer. In contrast, a primer strand containing 7D-2′E AMP did not support the incorporation of the next correct nucleotide. This demonstrates that 2′E-7D-ATP is an immediate chain terminator. This mechanism is very likely to explain the inhibition of dengue virus by beta-D-2′-ethynyl-7-deaza-adenosine.

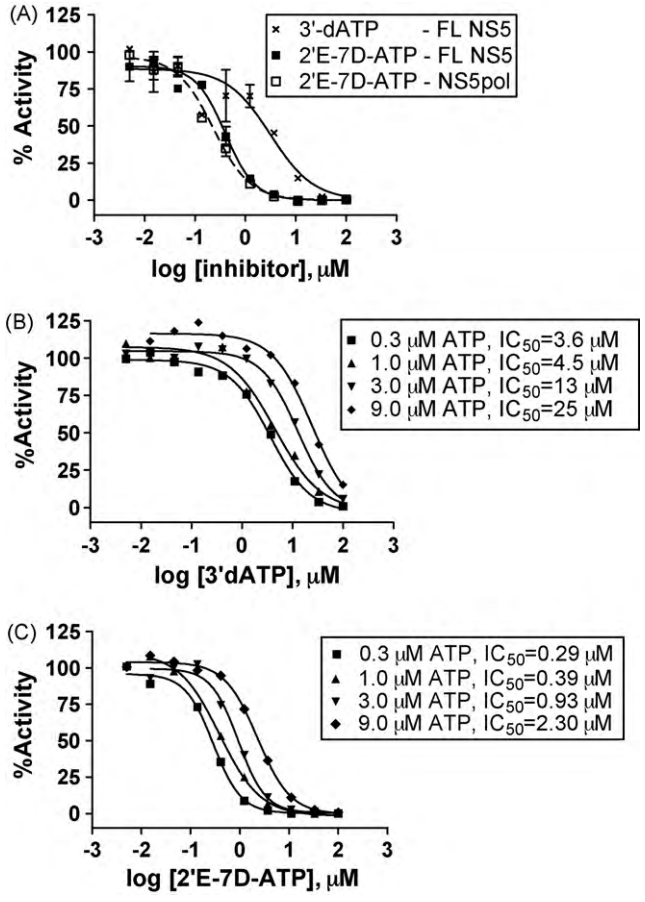

Fig. 4. Effect of the methyltransferase domain and ATP concentration on the inhibition of DENV-2 NS5 polymerase activity. (A) Inhibition of NS5pol domain and full-length NS5 by 2′E-7D-ATP and 3′dATP. (B) Dose–response for 3′-dATP against full-length NS5, in the presence of four different concentrations of natural ATP. K_i was calculated and averaged from each condition, using the Cheng–Prusoff equation (see Section 2). (C) same as (B) with 2′E-7D-ATP as the inhibitor of DENV-2 NS5.

3.5. Structural and genetic evidence for the conserved potency of 2′E-7D-ATP across the four serotypes of dengue virus

We modeled the positioning of 2′E-7D-ATP inside the active site of the dengue virus polymerase by superimposing the crystal structure of DENV-3 NS5 apo-protein with the crystal structure of bacteriophage Phi-6 polymerase containing a template strand, a nucleotide primer and the GTP substrate (Butcher et al., 2001; Yap et al., 2007). We aligned the conserved catalytic aspartates and immediately flanking regions of the two proteins before replacing the incoming nucleotide by 2′E-7D-ATP, opposite templated U (Fig. 6A). The model was refined by including the two coordinated metal ions, after superimposition with the ternary complex of HIV-1 reverse transcriptase (Huang et al., 1998). This allowed us to identify eleven residues neighboring the active site of DENV-3 NS5 polymerase domain that are within a perimeter of 5 Å from 2′E-7D-ATP (Fig. 6A). When we aligned the representative strains' sequences of the four serotypes, we observed that all eleven residues are perfectly conserved and belong to motifs A–D (Fig. 6B). In particular, a serine at position 600 (S600) is in the vicinity of the alkyne group at the 2′ position of the nucleotide. This serine is also conserved in HCV polymerase, where the mutation to a threonine induces resistance to 2′-methyl cytidine (Dutartre et al., 2006; Migliaccio et al., 2003). We created the counterpart S600T mutation in DENV-2 NS5. Compared to WT NS5, the S600T mutation induced a seven-fold loss in overall catalytic efficiency (Supplementary information Fig. 2). Most importantly, we observed the expected phenotypic loss of sensitivity to 2′E-7D-ATP (Fig. 6C). Overall, the combined information from the structural model, the sequence alignment, and the site-directed mutagenesis provide compelling evidence to explain the broad spectrum activity of beta-D-2′-ethynyl-7-deaza-adenosine across the four serotypes of dengue virus.

4. Discussion

Dengue fever is an emerging arbovirus disease for which no vaccine or antiviral are available (Damonte et al., 2004; Gubler, 1998; Halstead, 2007). In light of the recent progress made toward inhibiting essential steps of dengue virus replication, there are now reasons to believe that anti-dengue small molecules will soon enter clinical trials (Keller et al., 2006; Sampath and Padmanabhan, 2009). Success in drug discovery requires (1) the identification of molecular targets, (2) the design and validation of *in vitro* assays, and (3) the screen of potential hit-to-lead candidates. In this endeavor, virus entry, protease, and polymerase inhibitors have so far emerged as the most tractable classes of molecules against dengue virus (Lescar et al., 2008; Malet et al., 2008; Perera et al., 2008).

In this study, we report the detailed biochemical characterization of the inhibition of dengue polymerase by 2′E-7D-ATP. First, we compared the activity of all four serotypes of DENV NS5 under steady-state conditions of multiple nucleotide incorporations. NS5 from DENV-2 was 5- and 10-times more active than DENV-3 and DENV-4, respectively (Table 2). The least active protein in our hands was DENV-1 NS5, with only 1% of the catalytic efficiency of DENV-2 NS5. One limitation to this comparison is that the RNA template used in our standard assay is derived from the sequence of the New Guinea C strain of DENV-2, the same sequence that

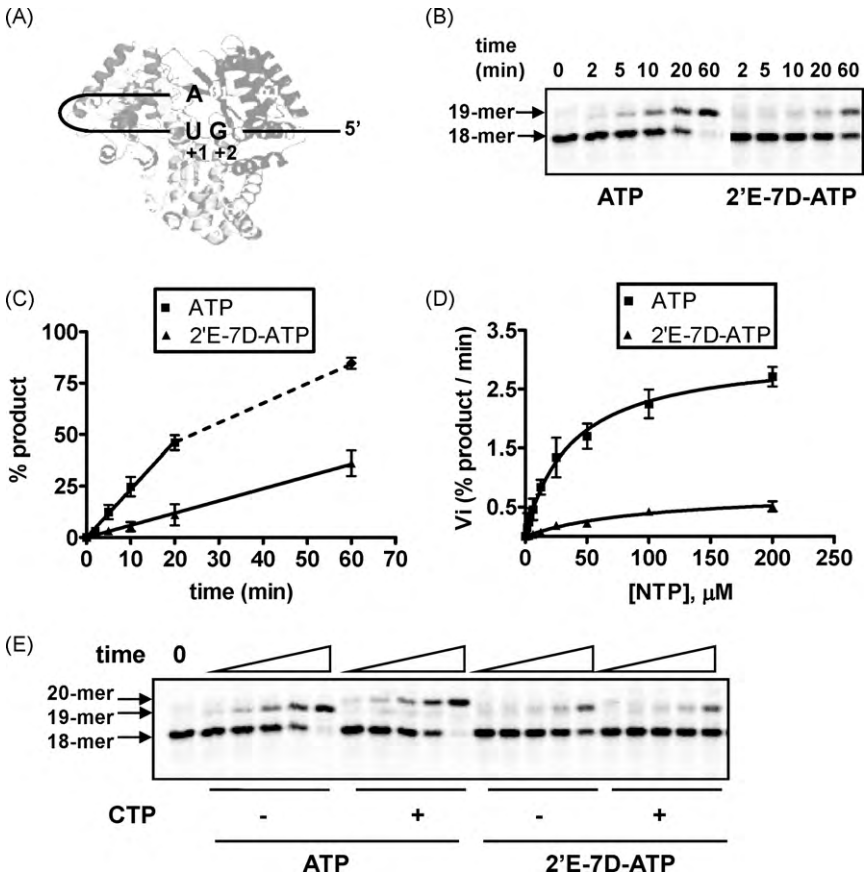

Fig. 5. Single beta-D-2′-ethynyl-7-deaza-AMP incorporation causes chain termination of RNA synthesis. (A) Schematic representation of single-nucleotide incorporation on a 18-mer hairpin-like RNA. Incorporation of an AMP at position +1 (opposite U) is followed by the next nucleotide C at position +2 (opposite G). (B) Time course of single-nucleotide incorporation. 100 μM of ATP (left) or 2′E-7D-ATP (right) were added to the polymerase reaction for 0, 2, 5, 10, 20, and 60 min with the conversion of 18-mer to 19-mer being tracked with 5′-end radiolabeled RNA, after separation of the two by sequencing PAGE analysis. ***C***, Relative representation of +1 product (19-mer) synthesis as percent product formed. The single-nucleotide reaction is linear for 20 min with ATP, and for at least 60 min with 2′E-7D-ATP. (D) Rate versus concentration plot analysis for ATP and 2′E-7D-ATP. Percent product formed is measured from a single time point of 10 min for ATP, and 60 min 2′E-7D-ATP. (E) Two-nucleotide incorporation experiments. AMP or 7D-2′E AMP at 100 μM is incorporated at position +1 (19-mer), alone, or in the presence of the next correct nucleotide CTP at 100 μM. Reaction times are 2, 5, 10, 20, and 60 min. Incorporation of two nucleotides is followed by the formation of a 20-mer product.

was used to generate the recombinant polymerase. In fact, it was recently suggested that NS5 recognizes a specific promoter element within the viral RNA, with important implications for the regulation of polymerase activity (Filomatori et al., 2006; Lodeiro et al., 2009). It would therefore be interesting to further assess the impact of RNA sequence on DENV NS5 polymerase activity. In this study, the same trend in polymerase activity between serotypes was observed using the homopolymeric poly(rA):oligo(rU) RNA substrate (Supplementary information Fig. 1B). In the case of serotype-1, we observed that the recombinant protein was less stable and more difficult to purify than the other serotype-derived NS5 proteins. Differences in protein stability or folding after expression may contribute to apparent differences in specific activity. It is therefore unclear how these distinct kinetic behaviors might translate at the level of virus replication. This could be addressed by further characterizing the polymerase activity of intact replicase complexes purified from infected cells. We also provided a comparative analysis of the specific activity between polymerase domain and full-length protein. In the presence of manganese, the two constructs displayed a similar rate of nucleotide incorporation, which is in agreement with a previous study (Selisko et al., 2006). We found that manganese primarily rescues the enzymatic activity of the polymerase domain (Fig. 2C), with less effect on the full-length enzyme that is already 20-times faster in the presence of magnesium. With this in mind, it would be interesting to further evaluate the contribution of the methyltransferase domain to initiation of RNA synthesis, an important step for the replication of the viral genome. While characterizing the catalytic activity of NS5, we also observed a 30- to 60-min lag phase under de-novo RNA synthesis conditions (Fig. 2A and Supplementary information Fig. 1A). This bi-phasic behavior might be attributed to the initial formation of pre-elongation complex before the system reaches equilibrium, as suggested by the quasi mono-phasic kinetics of polymerization measured in the presence of a primer (Supplementary information Fig. 1B). Since the reaction can be stopped at any time using heparin as a free-enzyme trap (data not shown), we believe that the rate of the linear phase is limited by initiation events.

Second, we showed that 2′E-7D-ATP inhibits the polymerase activity of both membrane-associated native DENV replicase as well as soluble recombinant NS5, which provides biochemical support for the inhibition of virus replication by the parent nucleoside (Tables 1 and 3). Under our conditions, 2′E-7D-ATP was about 10- to 15-times more potent than 3′-dATP, with an apparent K_i of 0.060 ± 0.016 μM against DENV-2 NS5. To the best of our knowledge, this makes beta-D-2′-ethynyl-7-deaza-adenosine the most potent nucleotide analogue against dengue polymerase reported to date (Olsen et al., 2004; Schul et al., 2007). The nucleobase modification enhanced the potency of the nucleotide, as demonstrated on dengue and HCV polymerase using the related 2′methyl-ATP (Supplementary information Fig. 3, Olsen et al., 2004). The K_i of 2′E-7D-ATP measured in the biochemical assay was about 10-fold lower than that of the EC_{50} of the parent nucleoside against dengue virus

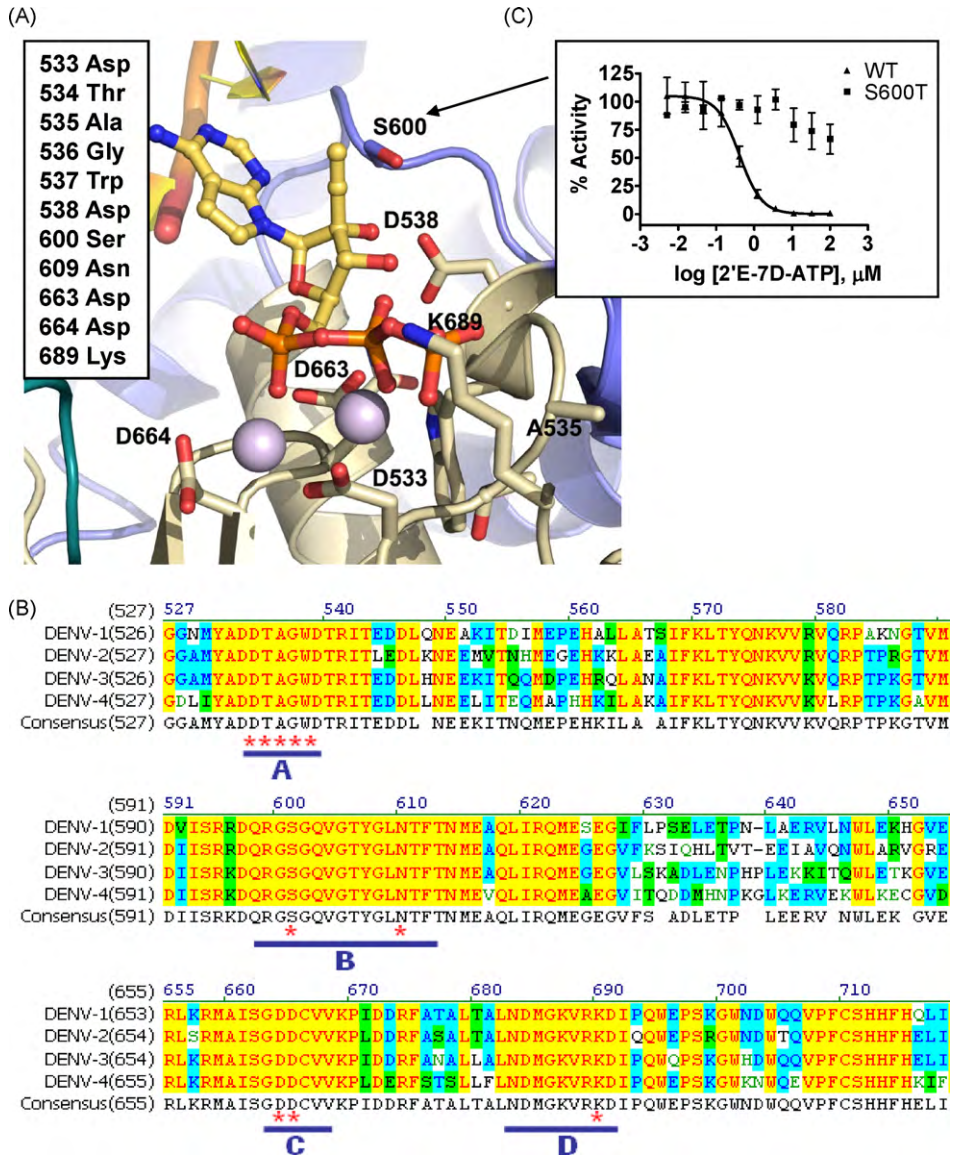

Fig. 6. Structural and genetic evidence for the conserved potency of 2′E-7D-ATP. (A) 2′E-7D-ATP was modeled inside the active site of the polymerase domain of NS5: PDB = 2J7U (Yap et al., 2007). The model was constructed by superimposition with the RNA polymerase of bacteriophage Phi-6 (PDB = 1HHT (Butcher et al., 2001)) providing a template strand orientation, and a complexed structure of HIV-1 RT (PDB = 1RTD (Huang et al., 1998)) to serve as a guide in positioning the two metal ions (purple) and the incoming nucleotide. Neighboring residues within 5 Å of the nucleotide binding site were selected (box). (B) Sequence alignment of the relevant portion of the four selected strains of dengue virus polymerase used in this study. The consensus sequence is also represented, and the 11 active site residues selected in (A) are highlighted with a red star. (C) Dose–response and IC_{50} determination for 2′E-7D-ATP against WT and S600T mutated DENV-2 NS5. The S600T variant was generated by site-directed mutagenesis.

in the cell-based assay. This apparent difference might be explained by nucleoside uptake and phosphorylation, two events that can limit the concentration of intracellular active triphosphate. Interestingly, our single-nucleotide incorporation experiments showed that 2′E-7D-ATP is a substrate of NS5 with a catalytic efficiency 10-fold lower than natural ATP (Fig. 5D). Therefore it should be possible to design other potent molecules at the level of polymerase binding and/or catalysis by further probing structure-activity relationship at the 2′-position, similarly to what has recently been done with 4′-modified ribonucleotides (Klumpp et al., 2008; Smith et al., 2007). Ultimately, a successful nucleoside drug candidate should combine favorable pharmacological properties starting with stability, permeability, activation through phosphorylation by cellular kinases, and finally with recognition by the viral target. We also show that 2′E-7D-ATP is potent against all four serotypes of dengue virus. The combined use of a structural model, sequence alignment, and site-directed mutagenesis provides compelling evidence to explain the broad spectrum activity of beta-D-2′-ethynyl-7-deaza-adenosine against dengue virus. In particular, the NS5 S600T mutant was able to discriminate against 2′E-7D-ATP, while remaining sensitive to 3'dATP. In single-nucleotide incorporation experiments with 400 μM 2′E-7D-ATP, less than 10% RNA product conversion was reached in 4 h by the S600T mutant (data not shown). This phenotype is reminiscent of the effect of the S282T mutation in HCV polymerase on the resistance to 2′-methylated nucleotides (Dutartre et al., 2006; Migliaccio et al., 2003). We predict that the conserved serine is likely to be in close proximity to the alkyne at 2′ position of the incoming nucleotide. In the case of dengue virus, we were not able to select any amino acid change at this position by resistance selection experiments with beta-D-2′-ethynyl-7-deaza-adenosine. Based on the reduced catalytic activity of the mutated enzyme (Supplementary information Fig. 2), we hypothesize that the mutation S600T might be too detrimental for dengue virus replication, as observed in the HCV replicon (Ludmerer et al., 2005).

At the time that this manuscript was prepared, Yin et al. (2009) published the antiviral activity of beta-D-2′-ethynyl-7-

deaza-adenosine in cultured cells against dengue virus and other *Flaviviruses* including HCV, yellow fever virus, West Nile virus, as well as in dengue infected animals. The authors also reported significant toxicity in rats and dogs when dosed for 2 weeks. The most noticeable side effect included decreased motor activity and blood abnormalities, which could not be predicted by *in vitro* experiments. There is a possibility that 2′E-7D-ATP is also a substrate for human polymerases. In the past, mitochondrial toxicity has been attributed to several nucleoside analogues inhibiting human DNA polymerase γ (Johnson et al., 2001; Lewis et al., 2003; Martin et al., 1994). Although we did not detect any apparent inhibition of human mitochondrial DNA polymerase γ *in vitro* (data not shown), we cannot exclude that beta-D-2′-ethynyl-7-deaza-adenosine interferes with lactic acid production or mitochondrial morphology. These particular studies, as well as potential bone marrow toxicity, should be conducted to investigate further the mechanism(s) of toxicity of beta-D-2′-ethynyl-7-deaza-adenosine. Overall, the undesirable effects reported by others underscore the difficulty to develop safe antivirals using nucleoside analogues, especially in order to treat chronic infections such as HIV or HCV. However, controlling acute infections such as the one inflicted by dengue virus could certainly benefit from short duration treatments with nucleosides.

5. Conclusions

In conclusion, our study provides biochemical evidence to suggest that modifying the ribose with an alkyne at the 2′ position offers a promising pharmacophore to inhibit NS5, the polymerase of dengue virus. 2′E-7D-ATP is a sub-micromolar inhibitor of NS5 from all four serotypes of dengue virus. Once incorporated into the growing RNA, 7D-2′E AMP causes immediate chain termination. These results warranty further evaluation of 2′ modified ribonucleotides against dengue virus and other members of the *Flaviviridae* family.

Acknowledgements

We thank Janice Bleibaum and Ken Straub for mass spectrometry analysis of protein sequence, and Han Ma for her help in setting up the *in vitro* replicase assay. YuYu Shu contributed to the early stages of this project.

Appendix A. Supplementary data

Supplementary data associated with this article can be found, in the online version, at doi:10.1016/j.antiviral.2010.05.003.

References

Ackermann, M., Padmanabhan, R., 2001. De novo synthesis of RNA by the dengue virus RNA-dependent RNA polymerase exhibits temperature dependence at the initiation but not elongation phase. J. Biol. Chem. 276, 39926–39937.

Bollati, M., Alvarez, K., Assenberg, R., Baronti, C., Canard, B., Cook, S., Coutard, B., Decroly, E., De Lambellerie, X., Gould, E.A., et al., 2009. Structure and functionality in flavivirus Ns-proteins: perspectives for drug design. Antiviral Res..

Bressanelli, S., Tomei, L., Roussel, A., Incitti, I., Vitale, R.L., Mathieu, M., De Francesco, R., Rey, F.A., 1999. Crystal structure of the RNA-dependent RNA polymerase of hepatitis C virus. Proc. Natl. Acad. Sci. U.S.A. 96, 13034–13039.

Brooks, A.J., Johansson, M., John, A.V., Xu, Y., Jans, D.A., Vasudevan, S.G., 2002. The interdomain region of dengue NS5 protein that binds to the viral helicase NS3 contains independently functional importin beta 1 and importin alpha/beta-recognized nuclear localization signals. J. Biol. Chem. 277, 36399–36407.

Butcher, S.J., Grimes, J.M., Makeyev, E.V., Bamford, D.H., Stuart, D.I., 2001. A mechanism for initiating RNA-dependent RNA polymerization. Nature 410, 235–240.

Choi, K.H., Groarke, J.M., Young, D.C., Kuhn, R.J., Smith, J.L., Pevear, D.C., Rossmann, M.G., 2004. The structure of the RNA-dependent RNA polymerase from bovine viral diarrhea virus establishes the role of GTP in de novo initiation. Proc. Natl. Acad. Sci. U.S.A. 101, 4425–4430.

Damonte, E.B., Pujol, C.A., Coto, C.E., 2004. Prospects for the therapy and prevention of dengue virus infections. Adv. Virus Res. 63, 239–285.

De Clercq, E., Neyts, J., 2009. Antiviral agents acting as DNA or RNA chain terminators. Handb. Exp. Pharmacol., 53–84.

Dutartre, H., Bussetta, C., Boretto, J., Canard, B., 2006. General catalytic deficiency of hepatitis C virus RNA polymerase with an S282T mutation and mutually exclusive resistance towards 2′-modified nucleotide analogues. Antimicrob. Agents Chemother. 50, 4161–4169.

Filomatori, C.V., Lodeiro, M.F., Alvarez, D.E., Samsa, M.M., Pietrasanta, L., Gamarnik, A.V., 2006. A 5′ RNA element promotes dengue virus RNA synthesis on a circular genome. Genes Dev. 20, 2238–2249.

Gubler, D.J., 1998. Dengue and dengue hemorrhagic fever. Clin. Microbiol. Rev. 11, 480–496.

Halstead, S.B., 2007. Dengue. Lancet 370, 1644–1652.

Huang, H., Chopra, R., Verdine, G.L., Harrison, S.C., 1998. Structure of a covalently trapped catalytic complex of HIV-1 reverse transcriptase: implications for drug resistance. Science 282, 1669–1675.

Johnson, A.A., Ray, A.S., Hanes, J., Suo, Z., Colacino, J.M., Anderson, K.S., Johnson, K.A., 2001. Toxicity of antiviral nucleoside analogs and the human mitochondrial DNA polymerase. J. Biol. Chem. 276, 40847–40857.

Keller, T.H., Chen, Y.L., Knox, J.E., Lim, S.P., Ma, N.L., Patel, S.J., Sampath, A., Wang, Q.Y., Yin, Z., Vasudevan, S.G., 2006. Finding new medicines for flaviviral targets. Novartis Found. Symp. 277, 109–114 (102–114, 251–103, discussion).

Klumpp, K., Kalayanov, G., Ma, H., Le Pogam, S., Leveque, V., Jiang, W.R., Inocencio, N., De Witte, A., Rajyaguru, S., Tai, E., et al., 2008. 2′-deoxy-4′-azido nucleoside analogs are highly potent inhibitors of hepatitis C virus replication despite the lack of 2′-alpha-hydroxyl groups. J. Biol. Chem. 283, 2167–2175.

Lescar, J., Luo, D., Xu, T., Sampath, A., Lim, S.P., Canard, B., Vasudevan, S.G., 2008. Towards the design of antiviral inhibitors against *Flaviviruses*: the case for the multifunctional NS3 protein from dengue virus as a target. Antiviral Res. 80, 94–101.

Lewis, W., Day, B.J., Copeland, W.C., 2003. Mitochondrial toxicity of NRTI antiviral drugs: an integrated cellular perspective. Nat. Rev. Drug Discov. 2, 812–822.

Lodeiro, M.F., Filomatori, C.V., Gamarnik, A.V., 2009. Structural and functional studies of the promoter element for dengue virus RNA replication. J. Virol. 83, 993–1008.

Ludmerer, S.W., Graham, D.J., Boots, E., Murray, E.M., Simcoe, A., Markel, E.J., Grobler, J.A., Flores, O.A., Olsen, D.B., Hazuda, D.J., et al., 2005. Replication fitness and NS5B drug sensitivity of diverse hepatitis C virus isolates characterized by using a transient replication assay. Antimicrob. Agents Chemother. 49, 2059–2069.

Ma, H., Leveque, V., De Witte, A., Li, W., Hendricks, T., Clausen, S.M., Cammack, N., Klumpp, K., 2005. Inhibition of native hepatitis C virus replicase by nucleotide and non-nucleoside inhibitors. Virology 332, 8–15.

Malet, H., Egloff, M.P., Selisko, B., Butcher, R.E., Wright, P.J., Roberts, M., Gruez, A., Sulzenbacher, G., Vonrhein, C., Bricogne, G., et al., 2007. Crystal structure of the RNA polymerase domain of the West Nile virus non-structural protein 5. J. Biol. Chem. 282, 10678–10689.

Malet, H., Masse, N., Selisko, B., Romette, J.L., Alvarez, K., Guillemot, J.C., Tolou, H., Yap, T.L., Vasudevan, S., Lescar, J., et al., 2008. The flavivirus polymerase as a target for drug discovery. Antiviral Res. 80, 23–35.

Martin, J.L., Brown, C.E., Matthews-Davis, N., Reardon, J.E., 1994. Effects of antiviral nucleoside analogs on human DNA polymerases and mitochondrial DNA synthesis. Antimicrob. Agents Chemother. 38, 2743–2749.

Migliaccio, G., Tomassini, J.E., Carroll, S.S., Tomei, L., Altamura, S., Bhat, B., Bartholomew, L., Bosserman, M.R., Ceccacci, A., Colwell, L.F., et al., 2003. Characterization of resistance to non-obligate chain-terminating ribonucleoside analogs that inhibit hepatitis C virus replication in vitro. J. Biol. Chem. 278, 49164–49170.

Olsen, D.B., Eldrup, A.B., Bartholomew, L., Bhat, B., Bosserman, M.R., Ceccacci, A., Colwell, L.F., Fay, J.F., Flores, O.A., Getty, K.L., et al., 2004. A 7-deaza-adenosine analog is a potent and selective inhibitor of hepatitis C virus replication with excellent pharmacokinetic properties. Antimicrob. Agents Chemother. 48, 3944–3953.

Perera, R., Khaliq, M., Kuhn, R.J., 2008. Closing the door on *Flaviviruses*: entry as a target for antiviral drug design. Antiviral Res. 80, 11–22.

Pryor, M.J., Rawlinson, S.M., Butcher, R.E., Barton, C.L., Waterhouse, T.A., Vasudevan, S.G., Bardin, P.G., Wright, P.J., Jans, D.A., Davidson, A.D., 2007. Nuclear localization of dengue virus nonstructural protein 5 through its importin alpha/beta-recognized nuclear localization sequences is integral to viral infection. Traffic 8, 795–807.

Ray, D., Shi, P.Y., 2006. Recent advances in flavivirus antiviral drug discovery and vaccine development. Recent Pat. Antiinfect. Drug Discov. 1, 45–55.

Sampath, A., Padmanabhan, R., 2009. Molecular targets for flavivirus drug discovery. Antiviral Res. 81, 6–15.

Schul, W., Liu, W., Xu, H.Y., Flamand, M., Vasudevan, S.G., 2007. A dengue fever viremia model in mice shows reduction in viral replication and suppression of the inflammatory response after treatment with antiviral drugs. J. Infect. Dis. 195, 665–674.

Selisko, B., Dutartre, H., Guillemot, J.C., Debarnot, C., Benarroch, D., Khromykh, A., Despres, P., Egloff, M.P., Canard, B., 2006. Comparative mechanistic studies of de novo RNA synthesis by flavivirus RNA-dependent RNA polymerases. Virology 351, 145–158.

Smith, D.B., Martin, J.A., Klumpp, K., Baker, S.J., Blomgren, P.A., Devos, R., Granycome, C., Hang, J., Hobbs, C.J., Jiang, W.R., et al., 2007. Design, synthesis, and antiviral properties of 4′-substituted ribonucleosides as inhibitors of hepatitis C virus replication: the discovery of R1479. Bioorg. Med. Chem. Lett. 17, 2570–2576.

Takeda, N., Kuhn, R.J., Yang, C.F., Takegami, T., Wimmer, E., 1986. Initiation of poliovirus plus-strand RNA synthesis in a membrane complex of infected HeLa cells. J. Virol. 60, 43–53.
van Dijk, A.A., Makeyev, E.V., Bamford, D.H., 2004. Initiation of viral RNA-dependent RNA polymerization. J. Gen. Virol. 85, 1077–1093.
Yap, T.L., Xu, T., Chen, Y.L., Malet, H., Egloff, M.P., Canard, B., Vasudevan, S.G., Lescar, J., 2007. Crystal structure of the dengue virus RNA-dependent RNA polymerase catalytic domain at 1.85-angstrom resolution. J. Virol. 81, 4753–4765.
Yin, Z., Chen, Y.L., Schul, W., Wang, Q.Y., Gu, F., Duraiswamy, J., Reddy Kondreddi, R., Niyomrattanakit, P., Lakshminarayana, S.B., Goh, A., et al., 2009. An adenosine nucleoside inhibitor of dengue virus. Proc. Natl. Acad. Sci. U.S.A. 106 (48), 20435–20439.
Yin, Z., Duraiswamy, J., Chen, Y.L. (2008) WO2008095993A1.